DISPERSION ANALYSIS OF A STRAIN-RATE DEPENDENT DUCTILE-TO-BRITTLE TRANSITION MODEL

HARM ASKES[1], JUHA HARTIKAINEN[2], KARI KOLARI[3], and REIJO KOUHIA[2]

[1] The University of Sheffield, Department of Civil and Structural Engineering Mappin Street, Sheffield, S1 3JD, UK
[2] Helsinki University of Technology, Structural Mechanics, P.O. Box 2100, FIN-02015 TKK
[3] VTT Technical Research Center of Finland, P.O. Box 1000, FIN-02044 VTT

ABSTRACT

Most materials exhibit rate-dependent inelastic behaviour. Increasing strain-rate usually increases the yield stress thus enlarging the elastic range. However, the ductility is gradually lost, and for some materials there exists a rather sharp transition strain-rate after which the material behaviour is completely brittle.

In this paper, a dispersion analysis of a simple phenomenological constitutive model for ductile-to-brittle transition of rate-dependent solids is presented. The model is based on consistent thermodynamic formulation using proper expressions for the Helmholtz free energy and the dissipation potential. In the model, the dissipation potential is additively split into damage and visco-plastic parts and the transition behaviour is obtained using a stress dependent damage potential.

1 INTRODUCTION

A large number of engineering materials, such as metals, polymers, concrete, soils and rock, can show reduction in the load carrying capacity accompanied by increasing localised deformations after the ultimate load is reached. If this phenomenon is considered as material property, it will lead to a negative slope of the stress-strain diagram, which is known as strain softening.

A demerit pertaining to strain-softening models for classical continua is that they result in problems which are not well-posed in general. The field equations of motion lose hyperbolicity and become elliptic as soon as strain softening occurs. The domain is split into an elliptic part, in which the waves are not able to propagate, and into a hyperbolic part with propagating waves. In static and quasi-static problems, localisation of deformation is usually understood as a synonym to the loss of ellipticity of the underlying rate-boundary value problem. When such problems are solved numerically, the solution of the localisation zone of zero thickness can result in mesh sensitivity. A simple remedy is to include viscous effects in the plastic model as proposed in [1]. Other improvements, e.g. [2, 3, 4, 5], are also possible. However, they usually involve additional field unknowns which make numerical computations more time-consuming. Also, the physical interpretation of the additional boundary conditions can be ambiguous.

In this study, a phenomenological model, which is capable of describing the strain-rate dependent ductile-to-brittle transition, is analysed. The ductile behaviour is considered as a viscoplastic feature, whereas the strain softening behaviour, after reaching the transition strain-rate, is dealt with

a continuum damage model. A dispersion analysis of the linearized equations of motion is carried out.

2 TRANSITION MODEL

The constitutive equations to model the ductile-to-brittle transition due to increasing strain-rate, are derived using a thermodynamic formulation, in which the material behaviour is described completely through the Helmholz free energy and the dissipation potential in terms of the variables of state and dissipation and considering that the Clausius-Duhem inequality is satisfied [6]. Detailed derivation of the model can be found in ref. [7]. The particular choice presented in ref. [7] can be described in a uniaxial case by the following constitutive equations, relating the stress σ, the elastic and inelastic strains, $\epsilon^{\mathrm{e}}, \epsilon^{\mathrm{i}}$, and the integrity or continuity, β as

$$\sigma = \beta E \epsilon^{\mathrm{e}} = \beta E \left(\epsilon - \epsilon^{\mathrm{i}}\right), \tag{1}$$

$$\frac{\mathrm{d}\epsilon^{\mathrm{i}}}{\mathrm{d}t} = \left[\frac{\varphi_{\mathrm{d}}}{(t_{\mathrm{vp}}^{\mathrm{ps}}\eta)^n \beta \sigma_{\mathrm{r}}}\left(\frac{|\sigma|}{\beta\sigma_{\mathrm{r}}}\right)^{np-1} + \frac{1}{t_{\mathrm{vp}}^{\mathrm{ps}}\beta}\left(\frac{|\sigma|}{\beta\sigma_{\mathrm{r}}}\right)^{p}\right] \mathrm{sign}\left(\frac{\mathrm{d}\epsilon}{\mathrm{d}t}\right), \tag{2}$$

$$\frac{\mathrm{d}\beta}{\mathrm{d}t} = -\frac{\varphi_{\mathrm{tr}}}{t_{\mathrm{d}}\beta}\left(\frac{Y}{Y_{\mathrm{r}}}\right)^{r}, \tag{3}$$

where the damage and transition parts of the dissipation potential are

$$\varphi_{\mathrm{d}} = \frac{1}{r+1}\frac{Y_{\mathrm{r}}}{t_{\mathrm{d}}\beta}\left(\frac{Y}{Y_{\mathrm{r}}}\right)^{r+1}, \tag{4}$$

$$\varphi_{\mathrm{tr}} = \frac{1}{pn}\left[\frac{1}{t_{\mathrm{vp}}^{\mathrm{ps}}\eta}\left(\frac{|\sigma|}{\beta\sigma_{\mathrm{r}}}\right)^{p}\right]^{n}. \tag{5}$$

The thermodynamic force Y, conjugate to the integrity flux is expressed as

$$Y = \frac{1}{2}E(\epsilon^{\mathrm{e}})^2 = \frac{1}{2E}\left(\frac{\sigma}{\beta}\right)^2. \tag{6}$$

The integrity β is related to the familiar damage parameter D by

$$\beta = 1 - D. \tag{7}$$

Parameters t_{d} and r, concern the damage evolution, the transition strain rate η and the exponent n the transition phase, and parameters $t_{\mathrm{vp}}^{\mathrm{ps}}$ and p the viscous behaviour. In addition E is the Young's modulus. The reference values σ_{r} and Y_{r} are arbitrary and here the following value for Y_{r} is chosen

$$Y_{\mathrm{r}} = \frac{\sigma_{\mathrm{r}}^2}{2E} = \frac{1}{2}E\epsilon_{\mathrm{r}}^2, \quad \text{where} \quad \epsilon_{\mathrm{r}} = \frac{\sigma_{\mathrm{r}}}{E}. \tag{8}$$

The transition function, φ_{tr}, deals with the change in the mode of deformation when the strain-rate $\mathrm{d}\epsilon^{\mathrm{i}}/\mathrm{d}t$ increases. In the viscous part, an overstress type of viscoplasticity [8, 9, 10] and the principle of strain equivalence [11, 12] are applied. The "pseudo"-relaxation time $t_{\mathrm{vp}}^{\mathrm{ps}}$ is related to the true relaxation time t_{vp} as

$$t_{\mathrm{vp}} = \epsilon_{\mathrm{r}} t_{\mathrm{vp}}^{\mathrm{ps}}. \tag{9}$$

The exponents $r, p \geq 0$ and $n \geq 1$ are dimensionless.

3 DISPERSION ANALYSIS

3.1 Non-dimensional form

Dispersion is the observation that harmonic waves, with a different wave length or frequency, propagate with different velocities. The ability to transform the shape of waves seems a necessary condition for continua to capture localisation phenomena. In a classical strain-softening solid, the waves are not dispersive, which means that the continuum is not able to transform propagating waves into stationary localisation waves [4]. In the dispersion analysis, a single linear harmonic wave is considered and the displacement field u for an infinitely long 1-D continuum has the form

$$u(x,t) = A\exp\left[i(kx-\omega t)\right], \tag{10}$$

in which k is the wave number and ω is the angular frequency.

The equation of motion for a uniform bar is

$$\rho\frac{\mathrm{d}^2u}{\mathrm{d}t^2} - \frac{\mathrm{d}\sigma}{\mathrm{d}x} = 0, \tag{11}$$

where ρ is the mass density of the material. For the dispersion analysis, the equations (11) and (1)-(3) are written in a non-dimensional form by defining the following non-dimensional quantities:

$$\tau = t/t_{\mathrm{e}}, \quad t_{\mathrm{e}} = L/c_{\mathrm{e}}, \quad \text{where} \quad c_{\mathrm{e}} = \sqrt{E/\rho}, \tag{12}$$

$$\xi = x/L, \quad \bar{u} = u/L, \quad s = \sigma/\sigma_{\mathrm{r}}, \tag{13}$$

where L is a typical characteristic length of the bar, and c_{e} is the speed of an elastic wave. In addition, it is convenient to define the relative strain

$$e = \epsilon/\epsilon_{\mathrm{r}}. \tag{14}$$

The following non-dimensional times are also used

$$\tau_{\mathrm{vp}} = t_{\mathrm{vp}}/t_{\mathrm{e}}, \quad \tau_{\mathrm{vp}}^{\mathrm{ps}} = t_{\mathrm{vp}}^{\mathrm{ps}}/t_{\mathrm{e}}, \quad \tau_{\mathrm{d}} = t_{\mathrm{d}}/t_{\mathrm{e}}. \tag{15}$$

Using the non-dimensional quantities, the equation of motion (11) takes the form

$$\ddot{\bar{u}} - \epsilon_{\mathrm{r}} s' = 0, \quad \text{where} \quad \ddot{\bar{u}} = \frac{\mathrm{d}^2\bar{u}}{\mathrm{d}\tau^2} \quad \text{and} \quad s' = \frac{\mathrm{d}s}{\mathrm{d}\xi}. \tag{16}$$

In the sequel, the superimposed dot represents the derivative w.r.t. the non-dimensional time τ and the prime the derivative w.r.t. the non-dimensional spatial coordinate ξ. If needed, the superimposed circle will denote the derivative w.r.t. real time, i.e.

$$\mathring{\epsilon} = \frac{\mathrm{d}\epsilon}{\mathrm{d}t}. \tag{17}$$

The constitutive equations (1)-(3) take the form

$$s = {\epsilon_{\mathrm{r}}}^{-1}\beta\epsilon^{\mathrm{e}}, \tag{18}$$

$$\dot{\epsilon}^{\mathrm{i}} = f(\beta, s), \tag{19}$$

$$\dot{\beta} = g(\beta, s) \quad \text{or} \quad \dot{\beta} = \tilde{g}(\beta, \epsilon^{\mathrm{e}}), \tag{20}$$

and the non-dimensional form of the wave is

$$\bar{u}(\xi,\tau) = \bar{A}\exp[i(\bar{k}\xi - \bar{\omega}\tau)]. \tag{21}$$

3.2 Viscous case

In the absense of damage the constitutive equations (1)-(3) reduce to

$$\dot{s} = {\epsilon_\mathrm{r}}^{-1}(\dot{\epsilon} - \dot{\epsilon}^\mathrm{i}), \tag{22}$$

$$\dot{\epsilon}^\mathrm{i} = \frac{1}{\tau_\mathrm{vp}^\mathrm{ps}} s^p. \tag{23}$$

In the equation of motion (16), the divergence of the stress at an arbitrary stress state s_* is

$$\dot{s}' = {\epsilon_\mathrm{r}}^{-1}\dot{\epsilon}' - \frac{p}{\epsilon_\mathrm{r}\tau_\mathrm{vp}^\mathrm{ps}} s_*^{p-1} s' = \epsilon_\mathrm{r}\dot{\epsilon} - as', \quad \text{where} \quad a = \frac{p}{\tau_\mathrm{vp}} s_*^{p-1}. \tag{24}$$

Taking time derivative of the equation of motion (16) and substituting the kinematical relation $\epsilon = \bar{u}'$ into the constitutive equations will result in the partial differential equation

$$\dddot{\bar{u}} - \dot{\bar{u}}'' + a\ddot{\bar{u}} = 0. \tag{25}$$

Substituting the waveform (21) into the equation (25) gives

$$i\bar{\omega}(\bar{\omega}^2 - \bar{k}^2) - a\bar{\omega}^2 = 0. \tag{26}$$

This equation can only be satisfied if the wavenumber is complex, i.e. $\bar{k} = \bar{k}_\mathrm{r} + \bar{\alpha}i$, which means that the harmonic wave is attenuated exponentially when traversing through the bar as

$$\bar{u}(\xi, \tau) = \bar{A}\exp(-\bar{\alpha}\xi)\exp[i(\bar{k}_\mathrm{r}\xi - \bar{\omega}\tau)]. \tag{27}$$

This will result in the dispersion relation

$$i\bar{\omega}(\bar{\omega}^2 - \bar{k}_\mathrm{r}^2 + \bar{\alpha}^2) + 2\bar{\omega}\bar{\alpha}\bar{k}_\mathrm{r} - a\bar{\omega}^2 = 0, \tag{28}$$

which has a solution

$$\bar{\omega} = \frac{\bar{k}_\mathrm{r}}{\sqrt{1 + \frac{1}{4}(a/\bar{k}_\mathrm{r})^2}}, \tag{29}$$

$$\bar{\alpha} = \frac{a}{\sqrt{2}\sqrt{1 + \sqrt{1 + (a/\bar{\omega})^2}}}. \tag{30}$$

The group and phase velocities c_R and c, respectively, are defined as

$$c_\mathrm{R} = \frac{\mathrm{d}\omega}{\mathrm{d}k_\mathrm{r}} = c_\mathrm{e}\frac{\mathrm{d}\bar{\omega}}{\mathrm{d}\bar{k}_\mathrm{r}} \quad \text{and} \quad c = \frac{\omega}{k_\mathrm{r}} = c_\mathrm{e}\frac{\bar{\omega}}{\bar{k}_\mathrm{r}}, \tag{31}$$

Notice that the group velocity is now larger than the phase velocity, a situation which is referred to as anomalous disperison ([13], p. 218).

The phase and group velocities and the damping coefficient as a function of the wavenumber k_r are shown in fig. 1 with different relative relaxation times and values of the exponent p at state $\sigma = \sigma_\mathrm{r}$. It can be seen that the waves are dispersive and the long waves are slowed down while the short waves are damped. Notice that the damping factor $\bar{\alpha}$ has the limit

$$\lim_{\bar{\omega}\to\infty} \bar{\alpha} = \tfrac{1}{2}a = \frac{p}{2\tau_\mathrm{vp}} s_*^{p-1}. \tag{32}$$

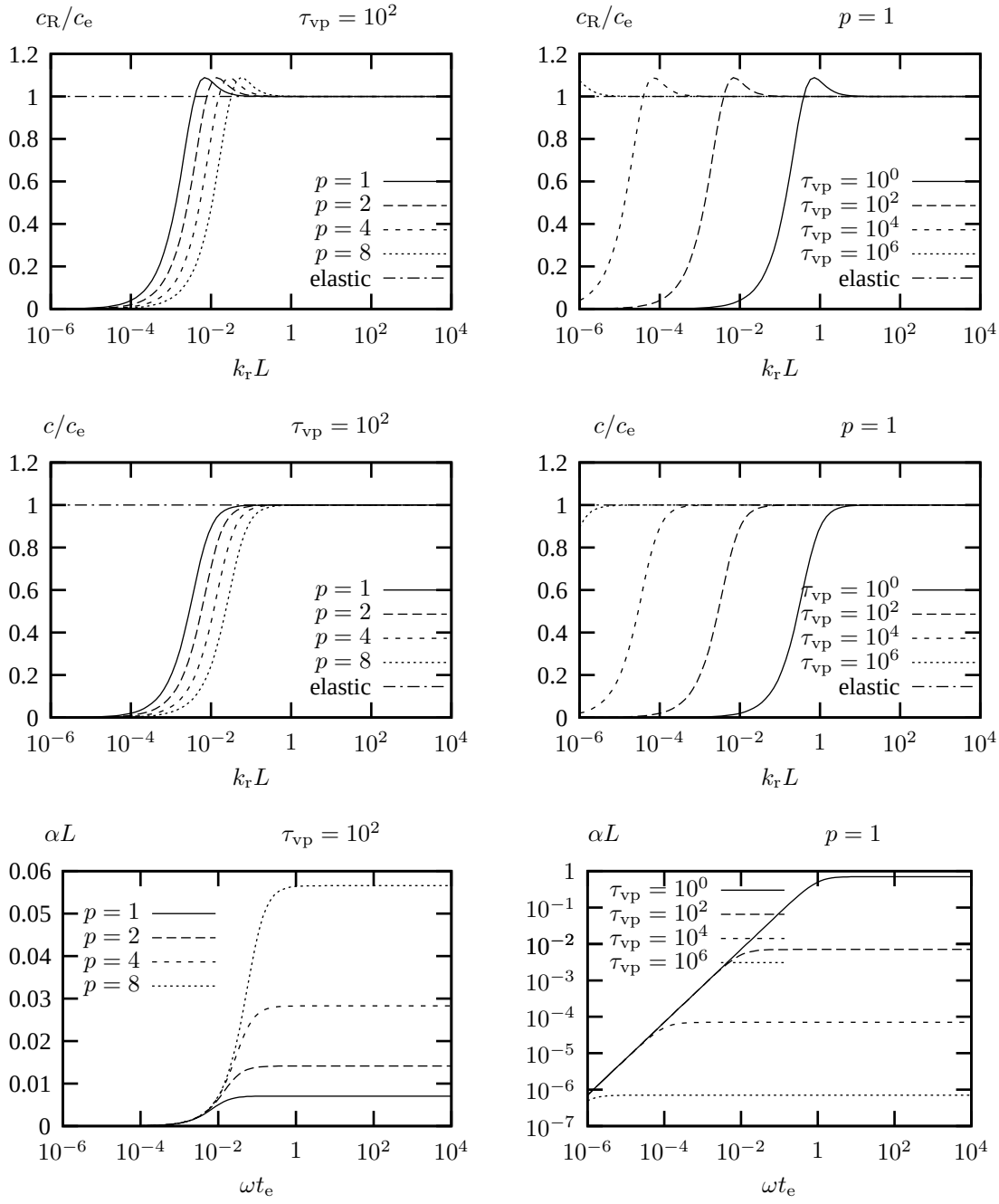

Figure 1: Viscous bar; group and phase velocity as a function of wavenumber and damping as a function of angular frequency.

3.3 Elasticity with damage

In the absense of viscous component the constitutive equations (1)-(3) reduce to

$$s = {\epsilon_\mathrm{r}}^{-1}\beta\epsilon = \beta e, \tag{33}$$

$$\dot{\beta} = -\frac{1}{\tau_\mathrm{d}}\beta^{-2r-1}s^{2r}, \tag{34}$$

and the non-dimensional equation of motion, linearized at state β_*, s_* is

$$\ddot{\bar{u}} - \epsilon_\mathrm{r} s' = \ddot{\bar{u}} - \epsilon_\mathrm{r}(\beta_*\dot{e}' + e_*\beta') = 0. \tag{35}$$

Divergence of the integrity rate is

$$\dot{\beta}' = g_1\beta' + g_2 s' = g_1\beta' + g_2{\epsilon_\mathrm{r}}^{-1}\ddot{\bar{u}}, \tag{36}$$

where

$$g_1 = \frac{2r+1}{\tau_\mathrm{d}}\beta_*^{-2r-2}s_*^{2r} \quad \text{and} \quad g_2 = -\frac{2r}{\tau_\mathrm{d}}\beta_*^{-2r-1}s_*^{2r-1}. \tag{37}$$

The elimination of β' results in

$$\dddot{\bar{u}} - h_0\dot{\bar{u}}'' - h_1\ddot{\bar{u}} + h_2\bar{u}'' = 0, \tag{38}$$

where

$$h_0 = \beta_*, \tag{39}$$

$$h_1 = g_1 + s_*\beta_*^{-1}g_2 = {\tau_\mathrm{d}}^{-1}\beta_*^{-2r-2}s_*^{2r}, \tag{40}$$

$$h_2 = \beta_* g_1 = (2r+1){\tau_\mathrm{d}}^{-1}\beta_*^{-2r-2}s_*^{2r}. \tag{41}$$

Substituting the expression for damped harmonic wave (27) into (38), yields

$$i\left[\bar{\omega}^3 - h_0\bar{\omega}(\bar{k}_\mathrm{r}^2 - \bar{\alpha}^2) - 2h_2\bar{k}_\mathrm{r}\bar{\alpha}\right] + 2h_0\bar{\omega}\bar{k}_\mathrm{r}\bar{\alpha} + h_1\bar{\omega}^2 - h_2(\bar{k}_\mathrm{r}^2 - \bar{\alpha}^2) = 0. \tag{42}$$

Since both the real and imaginary part of this expression has to vanish, it will result in two equations from which the wavenumber $\bar{k}_\mathrm{r}$ and the damping coefficient $\bar{\alpha}$ can be solved. After manipulations, resulting equations are

$${\bar{k}_\mathrm{r}}^4 - a_1\bar{k}_\mathrm{r}^2 - a_0^2\bar{\omega}^2 = 0, \quad \bar{\alpha} = a_0\bar{\omega}/\bar{k}_\mathrm{r}, \tag{43}$$

where

$$a_0 = \frac{(h_2 - h_0h_1)\bar{\omega}^2}{2(h_0^2\bar{\omega}^2 + h_2^2)}, \qquad h_2 - h_0h_1 = \frac{2r}{\tau_\mathrm{d}\beta_*}\left(\frac{s_*}{\beta_*}\right)^{2r}, \tag{44}$$

$$a_1 = h_0^{-1}(\bar{\omega}^2 - 2h_2a_0). \tag{45}$$

Clearly the term a_0 is positive, but the sign of the term a_1 depends on the state. Thus, the solution of (43) can be written as

$$\bar{k}_\mathrm{r}^2 = \tfrac{1}{2}|a_1|\left(\sqrt{1 + 4(a_0/a_1)^2} + \mathrm{sign}(a_1)\right). \tag{46}$$

The limit for the damping factor $\bar{\alpha}$ is

$$\lim_{\bar{\omega}\to\infty}\bar{\alpha} = \frac{h_2 - h_0h_1}{2h_0^2} = \frac{r}{\tau_\mathrm{d}\beta_*^3}\left(\frac{s_*}{\beta_*}\right)^{2r}. \tag{47}$$

The phase and group velocity as a function of the wavenumber at three instantaneous states are shown in fig. 2 for a constant strain rate loading case, the solution of which is:

$$\beta = \sqrt{1 - \frac{2}{2r+1}\frac{\epsilon_{\mathrm{r}}}{\overset{\circ}{\epsilon}_0 t_{\mathrm{d}}} e^{2r+1}}, \tag{48}$$

and $\overset{\circ}{\epsilon}_0$ is the constant loading rate. In the figure, the following value is used $\overset{\circ}{\epsilon}_0 t_{\mathrm{d}} = 10^{-2}$. The three states shown are (a) 19 % below the peak load $(e_* = 1.0, \beta_* = 0.9944, s_* = 0.9944)$, (b) at the peak load $(e_* = 1.364, \beta_* = 0.9045, s_* = 1.234)$ and (c) a softening region $(e_* = 1.5, \beta_* = 0.757, s_* = 1.135)$. The damping coefficient at these three stages is shown in fig. 4. It can be seen that the elastic damaging bar exhibits normal dispersion, i.e. $c_{\mathrm{R}} < c$.

At the peak load, the effect of parameter variations on the phase velocity is shown in fig.3 and on the damping coefficient in fig. 4 on the right-hand-side. The peak value of stress and the corresponding integrity value are

$$s_* = s_{\mathrm{peak}} = \left(\frac{2r+1}{2r+3}\right)^{\frac{2r+3}{4r+2}} \left(\frac{\overset{\circ}{\epsilon}_0 t_{\mathrm{d}}}{\epsilon_{\mathrm{r}}}\right)^{\frac{1}{2r+1}}, \quad \beta_* = \sqrt{\frac{2r+1}{2r+3}}. \tag{49}$$

3.4 Full model

The constitutive equations (1)-(3) reduce to

$$s = {\epsilon_{\mathrm{r}}}^{-1} \beta \epsilon^{\mathrm{e}} = \beta e^{\mathrm{e}}, \tag{50}$$

$$\dot{e}^{\mathrm{i}} = f(\beta, s) = \gamma_1 \beta^{-np-2r-3} s^{np+2r+1} + \gamma_2 \beta^{-p-1} s^p, \tag{51}$$

$$\dot{\beta} = g(\beta, s) = \gamma_3 \beta^{-np-2r-1} s^{pn+2r}, \tag{52}$$

where

$$\gamma_1 = \left[2(r+1)\tau_{\mathrm{d}}(t_{\mathrm{vp}}^{\mathrm{ps}}\eta)^n\right]^{-1}, \quad \gamma_2 = \tau_{\mathrm{vp}}^{-1} \quad \text{and} \quad \gamma_3 = -[pn\tau_{\mathrm{d}}(t_{\mathrm{vp}}^{\mathrm{ps}}\eta)^n]^{-1}. \tag{53}$$

Divergence of the inelastic strain rate and the integrity rate, linearized at state (β_*, s_*) can be represented as

$$\dot{e}^{\mathrm{i}\prime} = \frac{\partial f}{\partial \beta}|_* \beta' + \frac{\partial f}{\partial s}|_* s' = f_1 \beta' + f_2 s' = f_1 \beta' + f_2 \epsilon_{\mathrm{r}}^{-1} \ddot{\bar{u}}, \tag{54}$$

$$\dot{\beta}' = \frac{\partial g}{\partial \beta}|_* \beta' + \frac{\partial g}{\partial s}|_* s' = g_1 \beta' + g_2 s' = g_1 \beta' + g_2 \epsilon_{\mathrm{r}}^{-1} \ddot{\bar{u}}. \tag{55}$$

Eliminating β' will finally result in the equation

$$\dddot{\bar{u}} - h_0 \ddot{\bar{u}}'' - h_1 \ddot{\bar{u}} + h_2 \dot{\bar{u}}'' - h_3 \ddot{\bar{u}} = 0, \tag{56}$$

where

$$h_0 = \beta_*, \tag{57}$$

$$h_1 = g_1 + (s_*/\beta_*) g_2 - \beta_* f_2, \tag{58}$$

$$h_2 = \beta_* g_1, \tag{59}$$

$$h_3 = \beta_* (g_1 f_2 - f_1 g_2). \tag{60}$$

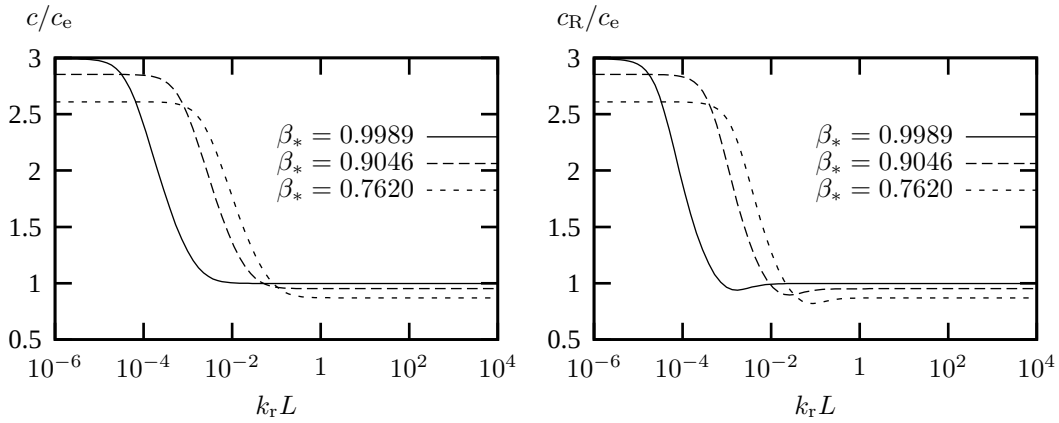

Figure 2: Elastic damaging bar; phase and group velocity as a function of wavenumber at different stages of the loading.

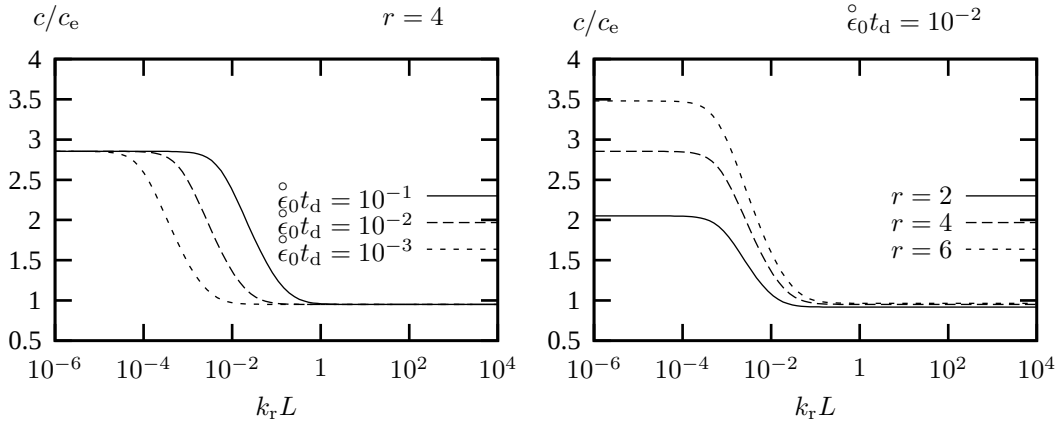

Figure 3: Elastic damaging bar; phase velocity as a function of wavenumber at the peak load with changing parameters.

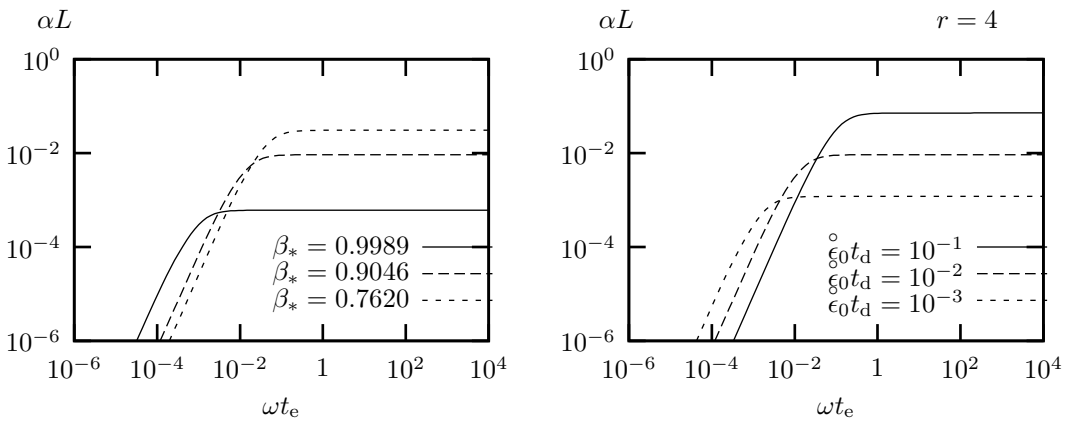

Figure 4: Elastic damaging bar; damping coefficient as a function of frequency at different stages of the loading: (l.h.s.) and with different values of the t_d-parameter at the peak load.

Table 1: Full transition model, the seven stages considered.

	1	2	3	4	5	6	7
e	0.100	0.400	0.700	0.900	1.100	1.500	2.500
s	0.100	0.400	0.697	0.888	1.067	1.110	0.718
β	1.000	1.000	1.000	1.000	0.999	0.913	0.612

The wavenumber $\bar{k}_{\mathrm{r}}$ and the damping coefficient $\bar{\alpha}$ can be solved from equations (43). In the full transition model, the coefficients in (43) have the forms

$$a_0 = \frac{(h_2 - h_0 h_1)\bar{\omega}^2 + h_2 h_3}{2(h_0^2\bar{\omega}^2 + h_2^2)}, \tag{61}$$

$$a_1 = h_0^{-1}(\bar{\omega}^2 - 2h_2 a_0 + h_3). \tag{62}$$

The behaviour of the coefficient a_0 for the full transition model (61) is different in comparison to the pure damage model (44). For the damage model a_0 is a positive, monotonously increasing function with the frequency attaining the zero value at vanishing frequency. In the full transition model, a_0 can have either positive or negative values. The limit values of a_0 are

$$a_{0,0} = \lim_{\bar{\omega}\to 0} a_0(\bar{\omega}) = \tfrac{1}{2}h_2^{-1}h_3 = \tfrac{1}{2}(f_2 - g_1^{-1}f_1 g_2), \tag{63}$$

$$a_{0,\infty} = \lim_{\bar{\omega}\to \infty} a_0(\bar{\omega}) = \tfrac{1}{2}h_0^{-1}(h_0^{-1}h_2 - h_1) = \tfrac{1}{2}(f_2 - \beta_*^{-2}s_* g_2) > 0. \tag{64}$$

The value of $a_{0,0}$ can be negative, which means that there exist a critical frequency $\bar{\omega}_{\mathrm{c}}$ when a_0 is zero, which gives zero value also for the wavenumber $\bar{k}_{\mathrm{r}}$, since it turns out that the coefficient a_1 is also negative. The special case of vanishing $\bar{k}_{\mathrm{r}}$ results the following form for the motion

$$\bar{u}(\xi,\tau) = \bar{A}\exp(-\bar{\alpha}\xi)\exp(-i\bar{\omega}_{\mathrm{c}}\tau), \tag{65}$$

which indicates a spatially varying but non-propagating disturbance.

In fig. 5, the stress-strain and integrity-strain curves are shown for a constant strain rate loading. The material parameters are those given in ref. [7], i.e. Young's modulus E = 40 GPa, Poisson's ratio $\nu = 0.3$, reference stress σ_{r} = 20 MPa, the viscoplastic pseudo relaxation time $t_{\mathrm{vp}}^{\mathrm{ps}} = 1000$ s and characteristic time for damage evolution $t_{\mathrm{d}} = 1$ s and the transition strain rate $\eta = 10^{-3}$ s^{-1}. All the exponents p, r and n have the value of 4. The loading strain-rate is ten times the transition strain rate.

The dispersion relation, phase velocity as and damping factor are presented in figs. 6-7 at the seven different stages indicated in fig. 5. The corresponding values of strain, stress and continuity are given in Table 1. The evolution of the critical frequency as a function of strain for different loading rates is shown in fig.8.

4 DISCUSSION AND CONCLUDING REMARKS

A dispersion analysis for a phenomenological constitutive model describing the ductile-to-brittle transition due to increased strain-rate is presented. Depending on the loading rate, the behaviour resembles either the behaviour of a viscous solid or an elastic-damaging solid. At strain-rates smaller

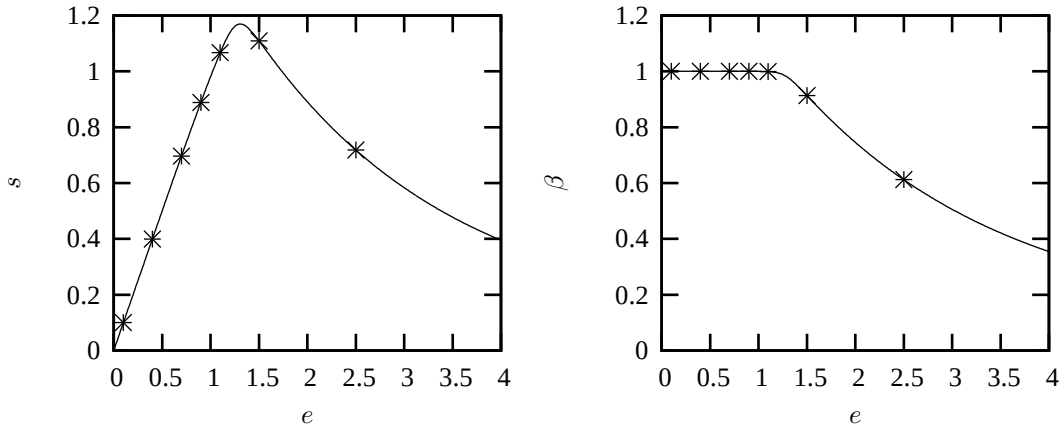

Figure 5: Stress-strain and integrity-strain curves. The seven considered stages are marked.

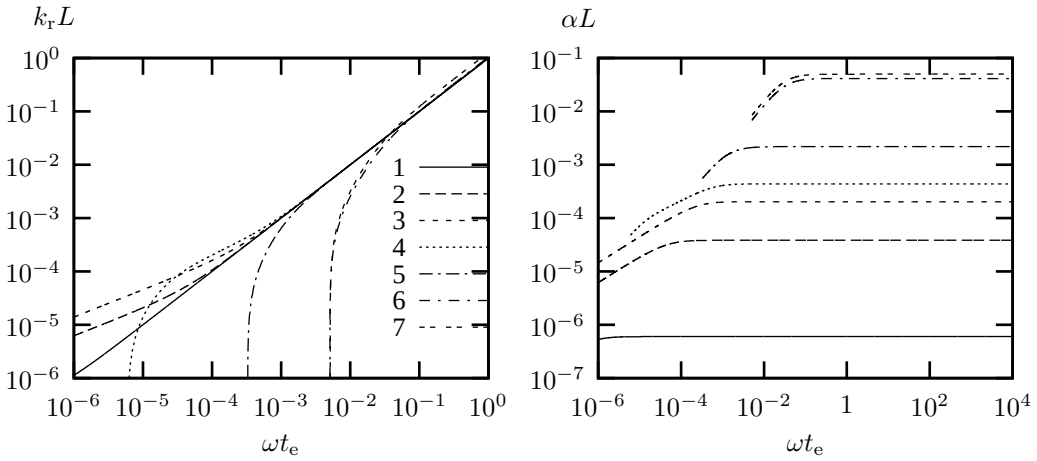

Figure 6: Full transition model; dispersion relation and the damping coefficient α as a function of frequency at different stages of the loading.

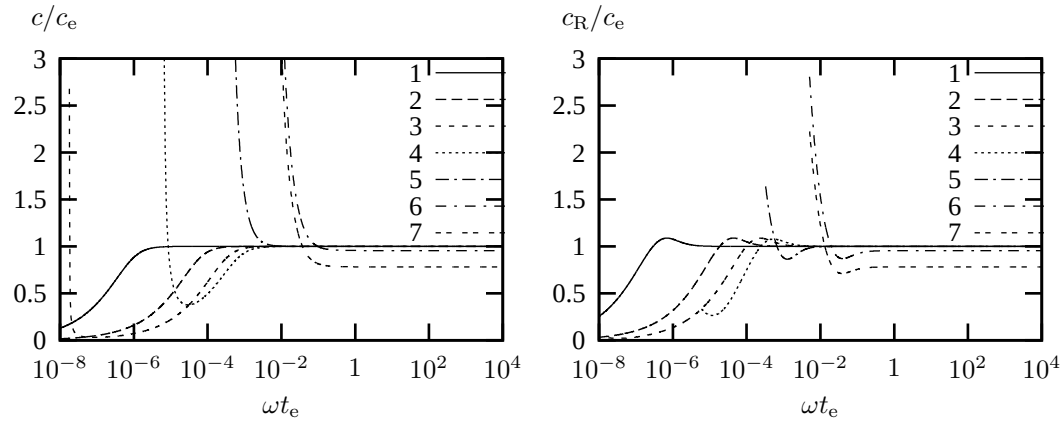

Figure 7: Full transition model; phase and group velocity c as a function of frequency at different load points.

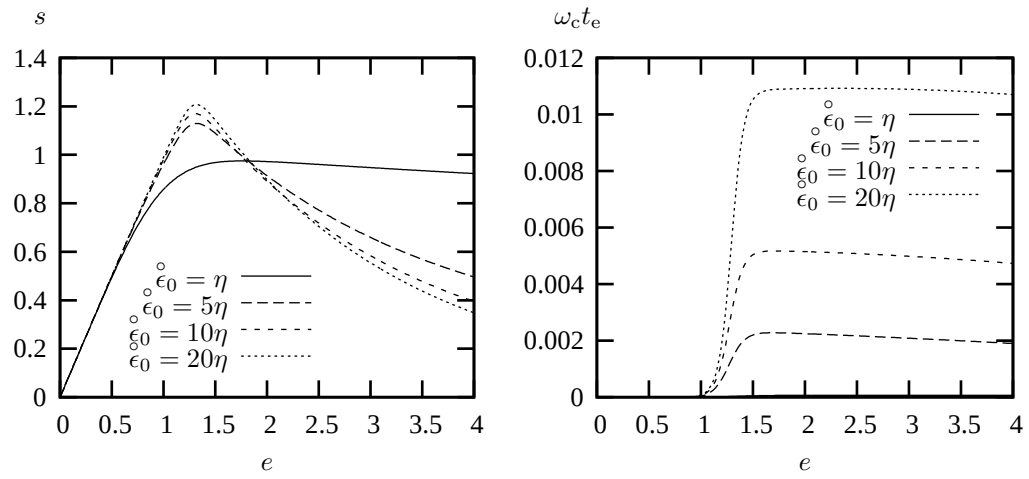

Figure 8: Stress-strain relation using different loading rate (l.h.s.) and evolution of the cut-off frequency with these loading rates (r.h.s.).

than the transition strain rate the behaviour is like in viscous solid; the phase- and group velocity approach the elastic wave speed at high frequences and vanish in the low frequency range. The dispersion is in such case of anomalous type. This is also true for higher strain-rates at the beginning of a loading process. For strain-rates higher than the transition strain-rate and states in the softening range, the behaviour is like elastic-damaging solid and the dispersion is of normal type. However, a rapidly growing critical frequency emerges near the maximum stress. At the intermediate states just before the peak load the dispersion is either anomalous or normal depending on the frequency (wavelength). As expected, the model is not able to slow down the high frequency components on the softening range. To obtain a model with such behaviour a higher-order continuum model is required [2].

At frequences higher than the critical frequency, the dispersion resembles a strain-softening viscoplastic solid. It is well known that viscosity introduces the material length scale in the model. An approximation to the width of the material length scale is (linearized from eq. (6.42) in Ref. [5]) $l_{\mathrm{mat}} \approx c_{\mathrm{s}} t_{\mathrm{vp}}^{\mathrm{ps}} \sigma_{\mathrm{r}} / (\frac{3}{4} G - h)$, where G is the shear modulus and $c_{\mathrm{s}} = \sqrt{G/\rho}$ is the elastic shear wave velocity and $-h$ is the softening modulus ($p = 1$). It should be mentioned that for softening viscoplastic solid, the width of the localisation zone could be dictated by the size of an imperfection. In a quasi-static loading the width of the localisation zone growns with increasing strain rate and enlarging material parameter p [14]. For the transition model for which the softening behaviour is due to the damage evolution, the situation might be different and is under investigation.

ACKNOWLEDGMENTS

This research has been supported in part by the Academy of Finland, decision number 121778.

REFERENCES

[1] A. Needleman. Material rate dependence and mesh sensitivity in localization problems, *Comp. Meth. Appl. Mech. Engng.*, **67**, 69–85 (1988).

[2] H. Askes, A.V. Metrikine. Higher-order continua derived from discrete media: continualisation aspects and boundary conditions. *Int. J. Solids Struct*. **42**(1), 187–202 (2005).

[3] A.C. Eringen. *Microcontinuum Field Theories, I. Foundations and Solids*, Springer, New-York, 1999.

[4] L.J. Sluys. *Wawe propagation, localisation and dispersion in softening solids*, PhD thesis, Department of Civil Engineering, Delft University of Technology, 1992.

[5] W. Wang. *Stationary and propagative instabilities in metals – a computational point of view*, PhD thesis, Department of Civil Engineering, Delft University of Technology, 1997.

[6] M. Frémond. *Non-Smooth Thermomechanics*, Springer, Berlin, 2002.

[7] S. Fortino, J. Hartikainen, K. Kolari, R. Kouhia and T. Manninen. A constitutive model for strain-rate dependent ductile-to-brittle transition. *The IX Finnish Mechanics Days*, 13-14.6.2006, Lappeenranta, Finland R. von Hertzen and T. Halme (eds.), pp. 652–662.

[8] P. Perzyna. Fundamental problems in viscoplasticity, *Advances in Applied Mechanics*, **9**, 243–377 (1966).

[9] G. Duvaut and L.J. Lions. *Inequalities in Mechanics and Physics*, Springer, Berlin, 1972.

[10] M. Ristinmaa and N.S. Ottosen. Consequences of dynamic yield surface in viscoplasticity, *Int. J. Solids Structures*, **37**, 4601–4622 (2000).

[11] J. Lemaitre, J.-L. Chaboche. *Mechanics of Solid Materials*, Cambridge University Press, 1990.

[12] J. Lemaitre. *A Course on Damage Mechanics*, Springer-Verlag, Berlin, 1992.

[13] J.D. Achenbach. *Wave propagation in elastic solids*. North-Holland series in applied mathematics and mechanics, Vol 16, 1973.

[14] K. Kolari, R. Kouhia and T. Kärnä. On viscoplastic regularization of strain softening solids. *The VIII Finnish Mechanics Days*, 12-13.6.2003, Espoo, Finland P. Råback, K. Santaoja and R. Stenberg (eds.), pp. 489–496.